Construction of a dynamic 4D probabilistic atlas for the developing brain

Maria Murgasova[a] Paul Aljabar[a] Latha Srinivasan[b] David Edwards[b] Jo Hajnal[b] Daniel Rueckert[a]

[a]Department of Computing, Imperial College London, [b]Department of Imaging Sciences, Imperial College London

Abstract. The segmentation of neonatal brain MR images is complicated by the rapid growth and by the changes in tissue properties which results in changing intensities of the brain tissue over time. In the light of these challenges the robustness of segmentation algorithms for neonatal brain MRI can be improved by including an age-specific spatial probabilistic atlas in the segmentation process. In this paper we describe a method for dynamically creating a probabilistic atlas for any chosen stage of development. The atlas is created from the brain images of 50 subjects of different ages using a kernel-based smoothing method. For any given age, an intensity template as well as the corresponding tissue probability maps with the correct sizes and shapes of the structures can be dynamically generated. This atlas improves the performance of standard segmentation techniques when applied to neonatal brain MRI.

1 Introduction

The role of robust automatic segmentation algorithms for neonatal brain MRI has become increasingly important as developments in neonatal medicine have improved the survival rates of prematurely born infants. The effects of premature birth on brain development still extend into later life [1], thus requiring a deeper understanding of the effect of prematurity on brain development. State-of-the-art techniques for brain MRI segmentation usually depend on spatial prior information in form of probabilistic atlas [2, 3]. While the between-tissue contrast is usually very good in the adult brains (after suitable intensity inhomogeneity correction), white matter (WM) in the neonatal brain exhibits high intensity variability due to process of myelination that gradually reverses the WM-GM contrast between the fifth month of pregnancy and one or two years of age. This substantial intensity variation increases the need for spatial prior information in order to improve the robustness of neonatal brain segmentation algorithms. However, the shapes and sizes of brain structures change at very fast rate before birth and during the first few months of life, due to rapid growth and the cortical folding process. We have developed a method for creating a dynamic 4D probabilistic atlas from a set of images acquired at different ages, which can be used to generate an age-specific atlas to improve neonatal brain segmentation. In recent years a number of neonatal segmentation methods have been proposed. Prastawa *et al.* [4] address the need for specific neonatal prior information by blurring an atlas constructed by averaging three affinely aligned manual segmentations. Weisenfeld *et al.* [5] segment images using an unbiased probabilistic atlas created by aligning 20 images with a group-wise registration method [6] and averaging their segmentations obtained by semi-automatic method [7]. All of the above methods use an atlas which is specific to subjects at term-equivalent age (approximately 40 weeks GA). An alternative approach has been proposed by Xue *et al.* [8] who develop a method for segmenting preterm infant brain MRI for various ages (27-42 weeks GA). In this method, a *quasi* probabilistic atlas is created for each subject by a k-means clustering and blurring process. In this paper we propose to build a new dynamic atlas which can be customized to build intensity templates and probabilistic priors for any given age and thus can improve robustness of neonatal segmentation methods.

2 Creating dynamic age-specific probabilistic atlases

Traditionally, probabilistic atlases are created from a large number of manually segmented anatomical images $I_1, ..., I_n$. The images are typically registered into a single reference space via affine transformations $A_1, ..., A_n$. The aligned images $I_k \circ A_k$ and corresponding segmentations for a label l, $S_{k,l} \circ A_k$, are then averaged to produce a probabilistic atlas. However, such an atlas is biased towards the reference space and may not represent the average geometry of the population. Much of this bias can be removed, if an average transformation $\bar{A}$ is used to estimate the average space atlas [9]. This is especially important for preserving correct sizes of the average neonatal atlases for different ages.

We represent affine transformation in 3D Euclidian space as 4×4 matrices acting on homogeneous coordinates. It is desired to average the affine transformations in relation to operation of composition $\circ$. The group of transformation with operation of composition does not form a vector space and average is therefore not defined. This can be overcome by estimating of the average for a set of affine matrices using matrix exponentials and logs:

$$\bar{A} = \exp(\frac{1}{n}\sum_{k=1}^{n}\log(A_k))$$

where matrix exponential and logarithm are defined via Taylor expansion. The details of the definition of addition and scaling operators as well as their implementation can be found in [10].

When building 4D atlas of growing brain, we aim to create a continuous set of templates dependent on a parameter t which represents time, or in our case the age of the subjects. This can be achieved by kernel regression, following the work of [11]. Let $t_1, ..., t_n$ be the gestational ages (GA) of the subjects at the time of scan. Then average transformation at the age t can be estimated as

$$\bar{A}(t) = \exp\left(\frac{\sum_{k=1}^{n} w(t_k, t)\log(A_k)}{\sum_{k=1}^{n} w(t_k, t)}\right)$$

We use a Gaussian kernel to calculate the weights

$$w(t_k, t) = \frac{1}{\sigma\sqrt{2\pi}} \exp^{\frac{-(t_k - t)^2}{2\sigma^2}}$$

The average template anatomy $\bar{I}(t)$ is then calculated as

$$\bar{I}(t) = \frac{\sum_{k=1}^{n} w(t_k, t) I_k \circ A_k \circ \bar{A}(t)^{-1}}{\sum_{i=1}^{n} w(t_k, t)} \tag{1}$$

and similarly a probability map $P_l(t)$ for tissue l is obtained by

$$P_l(t) = \frac{\sum_{k=1}^{n} w(t_k, t) S_{k,l} \circ A_k \circ \bar{A}(t)^{-1}}{\sum_{i=1}^{n} w(t_k, t)} \tag{2}$$

3 Segmentation of the training images

The following structures were used to create probabilistic atlases: Cerebro-spinal fluid (CSF), cortical WM, cortical GM, basal ganglia, brainstem and cerebellum. The central brain structures (basal ganglia, brainstem and cerebellum) tend to be well segmented by atlas-based segmentation where an atlas is propagated to the training images using non-rigid registration, such as [12]. We used a single manual segmentation of the reference subject as a deformable atlas.

In contrast, the segmentation of cortical structures and CSF using atlas-based segmentation is problematic, as it is extremely difficult to establish correspondences across cortical surfaces using intensity information alone. In the developing brain this is further complicated by the rapid process of cortical folding, the appearance and disappearance of CSF-filled spaces and the variation of intensity within WM. In particular the latter can cause intensity gradients that are not related to any structural boundaries. To avoid these problems we segment the cortical region based on intensity and adopt the algorithm developed by Xue *et al.* [8]. The advantage of this approach is the fact that it does not require any prior information in form of an atlas. Instead, a set of *quasi*-priors are estimated using k-means clustering at the beginning of the process. The EM-MRF segmentation [13] of WM, GM, and CSF is then performed with a modification of the MRF priors to correct partial volume (PV) misclassification on the CSF-GM and CSF-background boundaries. In our experience the algorithm performs well if there is good contrast between the tissue classes and little or no intensity inhomogeneity. However, if the assumptions are violated the algorithm tends to fail. Therefore, we have selected a suitable cohort of neonatal T2-weighted images with very good contrast and little or no intensity inhomogeneity. Any residual intensity inhomogeneity was corrected using a template-based bias correction method similar to the one proposed in [14]. An example of a segmentation using the above approach is shown in Fig. 1 (a).

4 Implementation and results

To create the 4D probabilistic atlas we used 50 T2-weighted fast-spin echo images acquired on 3T Philips Intera system with MR sequence parameters TR = 1712ms, TE = 160ms, flip angle 90° and voxel sizes $0.86 \times 0.86 \times 1$mm. The age range at the time of scan was 28 to 42 weeks (GA), with mean and standard deviation of 34 ± 4 weeks. All subjects were born prematurely.

We segmented all 50 images using the method described in Sec. 3. The chosen reference subject (36.3 weeks GA) was manually aligned to an orientation similar to ICBM152 atlas using only rigid transformation. In the first stage of the alignment, all the training images were aligned to the reference image using rigid registration. To achieve a meaningful rigid correspondence, only the central part of the reference subject, containing basal ganglia, ventricles and pons, was used to perform the initial rigid alignment. The central part of the brain in the reference subject was

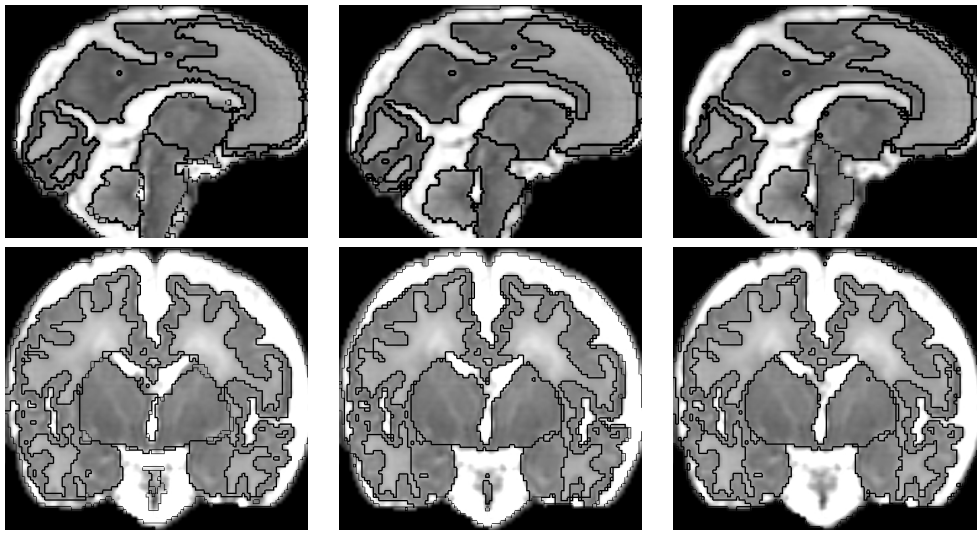

(a) (b) (c)

Figure 1. Segmentation of brain MRI of a baby scanned at 29 weeks (the first row) and 41 weeks (the second row) of gestation age. (a) Segmentation described in Sec. 3; (b) EM segmentation with non-rigidly aligned new probabilistic atlas; (c) EM-MRF-MLPV segmentation with non-rigidly aligned new probabilistic atlas.

delineated manually. This way we achieve good alignment of the structures that are very similar for all brains. In addition, we remove influence of cortical area and extra cranial CSF on the rigid alignment, as those vary substantially between subjects and can make resulting 4D dynamic atlas rotate or tilt with time, which is an undesirable artefact. In the second stage of the alignment, the rigidly aligned images were registered to the full reference subject to obtain affine transformations A_k which were then used to create age-specific templates and tissue probability maps using equations 1 and 2. We chose the standard deviation $\sigma = 2$ weeks. The resulting probability maps are shown in Fig. 2.

To evaluate the atlas, we segmented three images (GA 32, 35 and 38 weeks) which were not used to construct the atlas. The probabilistic atlases at the corresponding ages were non-rigidly aligned with each image using a registration algorithm based free-form deformations (FFDs) [12] using a control point spacing of 20mm. This coarse level of non-rigid registration was chosen due to the relatively blurry appearance of the intensity template. The EM segmentation method [13], which interleaves E-step (soft tissue classification and MRF estimation) with M-step (Gaussian distribution parameters estimation and bias field correction) was applied in two different ways: In the first version the algorithm was reduced to soft tissue classification and Gaussian distribution parameter estimation, while the MRF step and bias correction step were excluded (EM-atlas). In the second version the MRF estimation was included in the E-step, and correction of PV misclassification, as suggested by [8] was also incorporated (EM-MRF-MLPV-atlas). For comparison, combination of the method [8] and atlas-based segmentation, as described in Sec. 3 was also used *without* the atlas priors (EM-MRF-MLPV).

Fig. 1 shows the outcome of the three segmentation methods. All three segmentations were compared with manual segmentations of each image in four slices by computing the overlap of the segmentations as measured by the Dice coefficient [15]. The results indicate that the performance of all three methods is comparable (Table 1). The advantage of using a probabilistic atlas during the segmentation is that it improves the stability of the segmentation when the contrast between the tissues is not as good as for the training images used to build the atlas, which could be the case e.g. in fetal MR imaging. Additionally, using a probabilistic atlas removes the need for manual initialization of k-means clustering in EM-MRF-MLPV segmentation method [8]. The Fig.3 shows an example of failed EM-MRF-MLPV segmentation due to the incorrect convergence of k-means when constructing the quasi-prior. In contrast, the probabilistic atlas is a robust tool for correct initialization of EM segmentation.

Method	WM	Cortex
EM-MRF-MLPV	0.86 ± 0.03	0.75 ± 0.05
EM-atlas	0.84 ± 0.04	0.77 ± 0.03
EM-MRF-MLPV-atlas	0.84 ± 0.05	0.76 ± 0.03

Table 1. Overlap between manual and automatic segmentation of different segmentation methods.

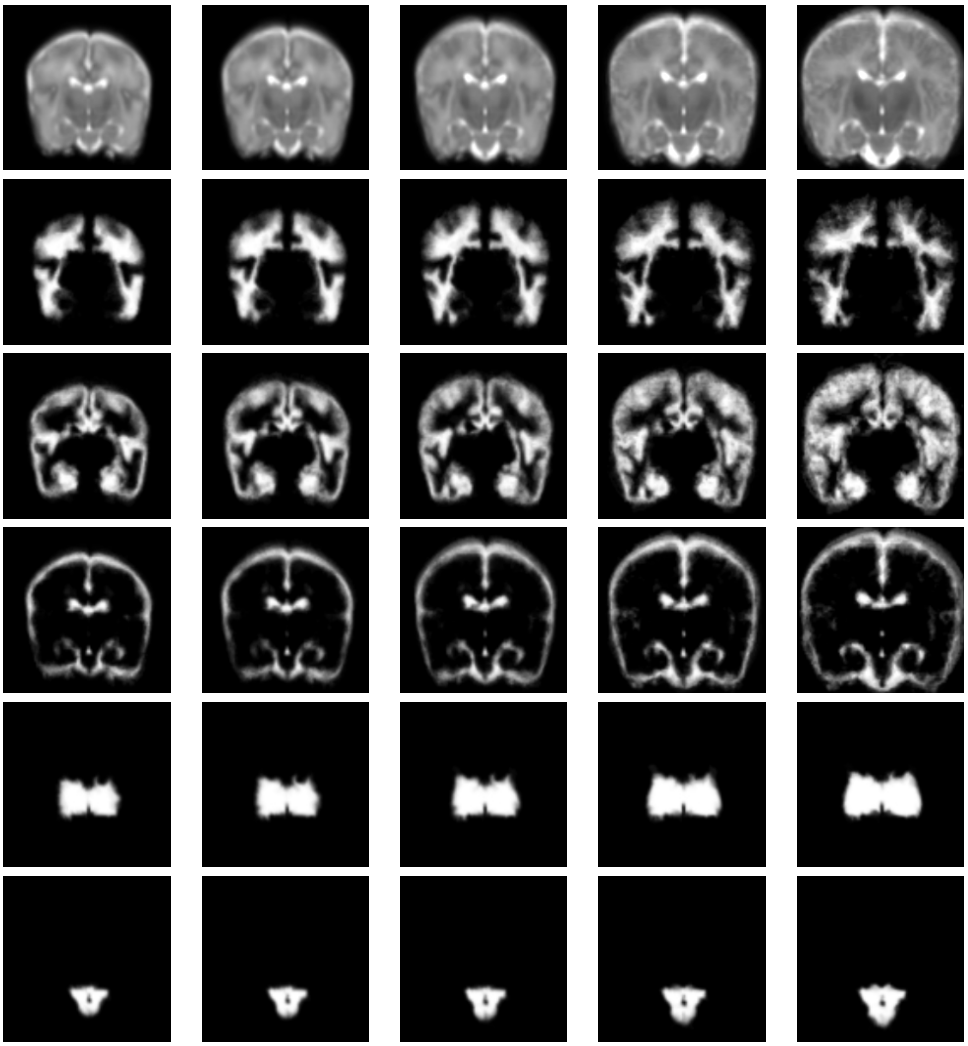

Figure 2. 4D dynamic probabilistic atlas of neonatal brain structures at ages of 29, 32, 35, 38, 41 weeks GA shown in columns from left to right. Structure probability maps shown in rows from top to bottom: intensity template, WM, cortical GM, CSF, basal ganglia, brainstem. The cerebellum not shown as it is not present in this slice.

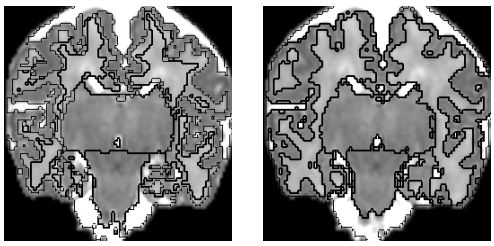

(a) (b)

Figure 3. Example of (a) failed segmentation by Xue *et al.* [8] and (b) good EM segmentation with non-rigidly aligned new probabilistic atlas.

5 Discussion

A dynamic probabilistic atlas is an important tool for the development of robust neonatal brain segmentation algorithms. In this work we used 50 subjects to produce the atlas, however, we plan to include more subjects in the study. Due to the rapid brain growth at this stage of development it is desirable to use as small standard deviations for the kernel smoothing as possible. When $\sigma = 2$ weeks was used, the number of images was sufficient to produce a smooth template at the earlier ages where the cortical part of the brain is still relatively simple. However, the template at 41 weeks, when cortex is already highly variable between individuals, exhibits quite a lot of individual features and does

not represent the average of the population sufficiently.

We have chosen to parcellate the brain in six structures. At this stage we have not modelled areas of myelinated WM explicitly. Tracking of the progress of myelination in the neonatal brain is a difficult problem due to the significant variability between subjects and the variation of WM intensities within a subject. We plan to address this issue using a combination of registration-based and intensity-based segmentation approaches. Between the ages 29 and 41 weeks GA most of the myelinated WM is contained within the basal ganglia, cerebellum and brainstem and therefore it does not cause significant misclassifications when using the constructed atlas priors.

Another issue to consider is the limitation of the segmentation method used in Sec. 3. The neonatal segmentation algorithms have to deal with significant challenges related to intensity variation within WM tissue, inevitably resulting in misclassifications. We found misclassifications at WM regions of very high intensity which lie in close proximity to ventricles and therefore resemble the CSF class, as well as partially myelinated regions of WM that are misclassified as cortical GM due to having a similar signal intensity. The algorithm described in [8] was shown to perform well compared to manual segmentations (Dice between 0.75 and 0.8), and can be therefore considered the state-of-the-art in neonatal segmentation. Segmentation errors are, however, transferred into probability maps. This issue could be addressed by perhaps including registration-based segmentation of WM and intracranial CSF (e.g. ventricles) when constructing probabilistic tissue maps. Nevertheless, the newly constructed templates substantially improve the performance of standard tools that use probabilistic atlases on neonatal data in comparison to using the adult or infant templates.

6 Conclusion

In this paper we presented a 4D dynamic probabilistic atlas for neonatal brain between ages 29 and 41 weeks GA. We have demonstrated that such an approach facilitates the use of standard segmentation methods which have been developed for adult brains and adopt these to neonatal brain segmentation. The resulting 4D dynamic atlas can be used as a step towards the development of robust segmentation tools for neonatal brains, which are still lacking in current literature.

References

1. N. Marlow, D. Wolke, M. Bracewell et al. "Neurologic and developmental disability at six years of age after extremely preterm birth." *Pediatrics* **115(2)**, pp. 286–94, 2005.
2. J. Ashburner & K. Friston. "Unified segmentation." *NeuroImage* **26**, pp. 839–851, 2005.
3. K. Pohl, J. Fisher, W. Grimson et al. "A Bayesian model for joint segmentation and registration." *NeuroImage* **31(1)**, pp. 228–239, 2006.
4. M. Prastawa, J. Gilmore, W. Lin et al. "Automatic Segmentation of Neonatal Brain MRI." In *Proc. of the 7th Int. Conf. on Medical Image Computing and Computer-Assisted Intervention, Part I*, pp. 10–17. 2004.
5. N. Weisenfeld, A. Mewes & S. Warfield. "Segmentation of newborn brain MRI." In *Proceedings of IEEE International Symposium on Biomedical Imaging*, pp. 766–769. 2006.
6. L. Zöllei. *A Unified Information Theoretic Framework for pair- and Group-wise Registration of Medical Images.* Ph.D. thesis, MIT, 2006.
7. S. Warfield, M.Kaus, F. Jolesz et al. "Adaptive template moderated spatially varying statistical classification." In *Proc. of the 1st Int. Conf. on Medical Image Computing and Computer-Assisted Intervention*, pp. 431–438. 1998.
8. H. Xue, L. Srinivasan, S. Jianga et al. "Automatic segmentation and reconstruction of the cortex from neonatal mri." *NeuroImage* **38(3)**, pp. 461–477, 2007.
9. A. Guimond, J. Meunier & J. Thirion. "Average brain models: a convergence study." *Computer vision and image understanding* **77**, pp. 192–210, 2000.
10. M. Alexa. "Linear combination of transformations." *ACM Trans. Graph.* **21(3)**, pp. 380–387, 2002.
11. B. Davis, P. Fletcher, E. Bullitt et al. "Population shape regression from random design data." In *International Conference on Computer Vision*. 10 2007.
12. D. Rueckert, L. Sonoda, C. Hayes et al. "Non-rigid registration using free-form deformations: Application to breast MR images." *IEEE Transactions on Medical Imaging* **18(8)**, pp. 712–721, 1999.
13. K. V. Leemput, F. Maes, D. Vandermeulen et al. "Automated model-based tissue classification of MR images of the brain." *IEEE Transactions on Medical Imaging* **18(10)**, pp. 897–908, 1999.
14. M. Murgasova, J. Hajnal, S. Counsell et al. "Template-based bias correction: Application to paediatric brain MRI." In *ISMRM*, p. to appear. 2009.
15. L. Dice. "Measures of the amount of ecologic association between species." *Ecology* **26**, pp. 297–302, 1945.